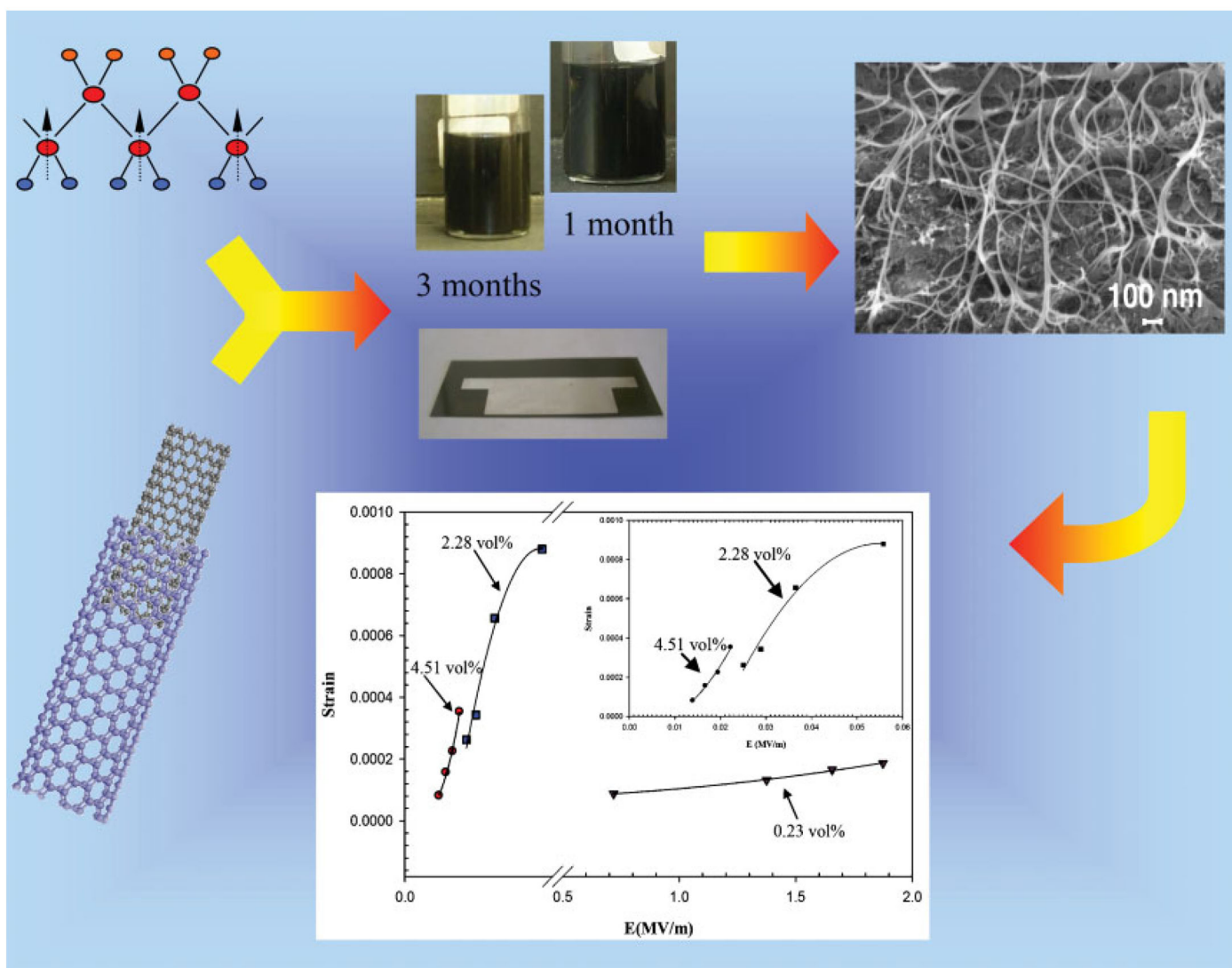




Macromolecular Materials and Engineering

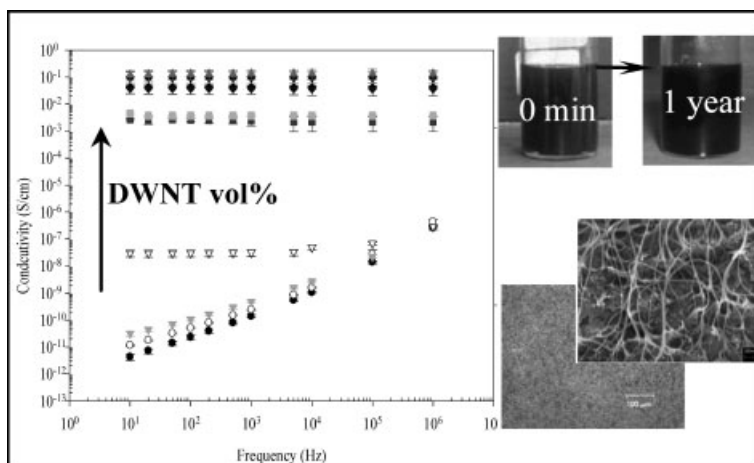


2/2008

Characterization of Solution-Processed Double-Walled Carbon Nanotube/ Poly(vinylidene fluoride) Nanocomposites

Atheer Almasri, Zoubeida Ounaies,* Yeon Seok Kim, Jaime Grunlan

Dispersion of CNTs in polymers can yield impressive property enhancements at low volume fractions, thus maintaining the inherent processability of the polymer. In particular, they can improve the electromechanical response of piezoelectric polymers by lowering the actuation voltage and increasing strain and stress response. In this work, piezoelectric PVDF and DWNTs are solution-cast into films. SEM of fracture surfaces confirms good dispersion, and electrical conductivity measurements reveal a low percolation threshold (0.23 vol.-%). The effect of CNTs on storage modulus, T_c , T_m and T_g of PVDF is studied. Electromechanical strain is observed at low actuation voltages, possibly due to enhanced local electric field in the presence of DWNTs.



Introduction

Carbon nanotube (CNT)/polymer composites are of great interest due to the unusual combination of CNT properties with apparently paradoxical attributes such as high

strength and modulus yet high flexibility, relatively high elongation at break, and low density, rendering them very unique inclusions that would improve properties of polymers yet still preserve their advantages such as ease of processing, light weight, and flexibility.^[1–5] Gojny et al. investigated the effect of adding small amounts of double-walled nanotubes (DWNT) on the mechanical properties of an epoxy. At 0.1 wt.-% nanotubes content, both the tensile strength and the Young's modulus increased while ductility was retained.^[4] Pötschke et al. reported a significant increase in the conductivity and the dielectric constant of a polycarbonate composite by adding multi-walled carbon nanotubes (MWNTs).^[5] The percolation concentration, the threshold below which the composite is insulating and above which it is conductive, was calculated to be 1.0 wt.-% for the MWNTs. Ounaies

A. Almasri, Z. Ounaies

Aerospace Engineering Department, 3141 TAMU, Texas A&M University, College Station, TX 77843, USA

Fax: +1 979 845 6051; E-mail: zounaies@tamu.edu

Y. S. Kim, J. Grunlan

Mechanical Engineering Department, 3141 TAMU, Texas A&M University, College Station, TX 77843, USA

A. Almasri, Z. Ounaies, J. Grunlan

Materials Science and Engineering Program, 3141 TAMU, Texas A&M University, College Station, TX 77843, USA

et al. reported that the dielectric constant and the AC and DC conductivity were enhanced by ten orders of magnitude by using single-walled carbon nanotubes (SWNT) in a polyimide matrix.^[6] The percolation threshold was found to be 0.05 wt.-% SWNT. All of these improvements are obtained at very low filler contents, highlighting that improvement of the polymer properties does not come at the expense of processability. Dispersion of the nano-inclusions in the polymer matrix remains a challenge. Intrinsic van der Waals attraction in combination with high surface area leads to significant agglomeration and clustering. Although a number of studies have focused on dispersion of CNT in polymers, complete dispersion of CNT in a polymer matrix remains elusive. Most published work has focused on chemical modification of the CNT to improve dispersion through functionalization.^[7–9] Functionalization may improve efficiency of load transfer between the polymer and the CNT, however, it also introduces defects on the CNT walls, which will lower their inherent properties such as electrical and thermal conductivity. Other researchers have investigated non-covalent means of dispersing the CNTs in polymers.^[10–12] Wise et al. identified a donor-acceptor interaction between CNT and a polar polyimide, which promotes a homogeneous dispersion of the CNTs through non-covalent bonding.^[13] Their finding suggests an interaction between CNTs and dipolar groups in polymers.

Combining a piezoelectric polymer poly(vinylidene fluoride) (PVDF) with embedded CNTs may lead to improvements in sensing and actuation. PVDF is the only commercially available piezoelectric polymer and has the highest piezoelectric coefficient among the synthetic polymers.^[14,15] PVDF is typically 50–60% crystalline depending on the thermal and processing history, and has four crystal phases (α , β , γ , and δ), three of which are polar. The most stable is the non-polar α phase which forms upon casting PVDF from the melt. The α phase can be transformed into the polar β phase by mechanical stretching at elevated temperatures. The β phase displays the highest value of dipole moment (≈ 2.1 Debye), making it the most important phase for piezoelectric considerations.^[14] In the β form, PVDF is suitable for sensor and actuator applications due to its low density, flexibility, and elastic modulus.

In the present work, DWNT/PVDF composites are prepared to assess the quality of nanotube dispersion and the resulting physical properties. DWNTs are a special case of multi-walled carbon nanotubes (MWNTs) that are not sufficiently studied and consequently there is a need to understand their properties. In contrast to MWNTs, where a batch is constituted of tubes with different numbers of walls, DWNTs have two layers of tubes so the effect of the walls can be more precisely analyzed, allowing for the possibility to validate and later predict results using

computational approaches. As compared to SWNTs, the advantages of DWNTs are linked to their availability and lower cost. Furthermore, the outer tube of a DWNT can be functionalized (either covalently or non-covalently), leaving the inner tube pristine, therefore effectively conserving the inherent electrical properties. We have dispersed DWNTs in PVDF, using no surfactant, by relying on previously established non-covalent interactions between the tubes and the PVDF polymer structure.^[16] Indeed, Owens et al. reported an interaction between SWNT and PVDF, demonstrated by a shift in Raman peaks, which indicates a donor-acceptor interaction between the SWNTs and the fluorine dipole in PVDF. We also assessed the effect of adding the DWNTs on the piezoelectricity of PVDF. Scanning electron microscopy (SEM) was used to qualitatively probe the dispersion resulting from this solution-based processing method. Electrical conductivity techniques were used to investigate the dispersion quantitatively through measuring the percolation threshold concentration for this nanocomposite. Both the electrical conductivity (σ) and the dielectric constant (ϵ) were measured as a function of frequency and content of DWNT. DSC measurements were done to study the influence of adding DWNT on the melting temperature (T_m), the glass transition temperature (T_g) and the degree of crystallinity of the PVDF matrix. Finally, electromechanical measurements are done to assess the electromechanical behavior of the DWNT/PVDF composites.

Experimental Part

Composite Preparation

DWNT were provided by Carbon Nanotechnologies Inc. (Houston, TX). As per the manufacturer's product sheet, the radius range of the DWNTs was 0.75–1.5 nm, and the length range was 200–2 000 nm. PVDF powder (tradename Kynar 500) was provided by Arkema Inc. (King of Prussia, PA). Kynar 500 is a high molecular weight, low crystallinity form of PVDF. The set-up consists of a three-neck flask equipped with a nitrogen inlet and outlet, a mechanical stirrer and a sonicator operated at a frequency of 40 kHz. Anhydrous *N,N*-dimethylacetamide (DMAc) with a purity of 99.8%, from Sigma-Aldrich (Milwaukee, WI), was used as the solvent. A given weight of DWNTs was placed in the flask and dispersed in DMAc. The flask was put in a sonicator after connecting it to a mechanical stirrer at 100 rpm. Simultaneous stirring and sonication was carried out for 1 h. The stirrer speed was then increased to 150 rpm for 1 h, followed by 1 h at 200 rpm to complete the procedure. Finally, PVDF was added to the DWNT/DMAc solution in the flask and the whole solution was stirred at 150 rpm under sonication for 1 h. At the end of this hour, sonication was turned off and the solution was mechanically stirred for 9 h. The detailed procedure is summarized in Table 1, and was adapted from dispersing SWNT in a polyimide matrix.^[17] After 9 h, the solution was placed in a vacuum oven at room temperature for 5 min. This step is necessary to remove the

Table 1. Procedure for dispersion of DWNTs in PVDF.

Solution	Mechanical stirrer speed	Sonicator state	Time
	rpm		
DWNT	100	On	1
DWNT	150	On	1
DWNT	200	On	1
DWNT/PVDF	150	On	1
DWNT/PVDF	150	Off	9

bubbles that form in the solution. A doctor blade is used to cast the solution on a glass plate. The glass plate is put in a desiccator for 24 h until the film is tack-free, then 3 h in a vacuum oven at 40 °C to fully evaporate the solvent. The same procedure was followed for all concentrations used in this study.

Composite Characterization

The SEM images of the composites were obtained using a Zeiss 1530 VP FE-SEM. For SEM imaging, DWNT composite samples are initially frozen in liquid nitrogen, then fractured and coated with platinum. Electrical conductivity and dielectric constant were measured under a parallel plate configuration for all samples using a QuadTech 7000 LCR high precision meter (Maynard, MA). The frequency range for this instrument is 10 Hz to 2 MHz. DSC was performed using a Mettler Toledo DSC 821 (Columbus, OH) from 30 to 200 °C at a heating rate of 10 K · min⁻¹ with nitrogen as the purge gas (80 mL · min⁻¹) for the first heating cycle. A TA instrument RSA II dynamic mechanical analyzer (DMA) (New Castle, DE) was used to measure mechanical properties of DWNT/PVDF nanocomposite films. Measurements were done at 1 Hz frequency between -100 and 150 °C at a rate of 2 K · min⁻¹ in tension mode. Strain was measured by first cutting strips of 3 × 0.5 cm², and depositing a thin silver layer (≈100 nm) using a metal evaporator. The top of the sample was then sandwiched between glass plates in a cantilevered beam configuration. The experiment was performed in a transparent acrylic box to protect the sample from the environment. Leads from the sample were connected to a power supply and the movement of the film was captured by a fast speed camera. The images were analyzed using Photron (San Diego, CA) image analysis software where the tip displacement is measured and related to the extensional strain.

Results and Discussion

DWNT Dispersion and Microstructure

Figure 1 shows DWNT/PVDF solutions in glass vials taken over a period of time up to one year after the solution was prepared. No settling or segregation of the DWNTs is observed, indicating a long term stable dispersion of DWNTs in the PVDF solution. As mentioned earlier,

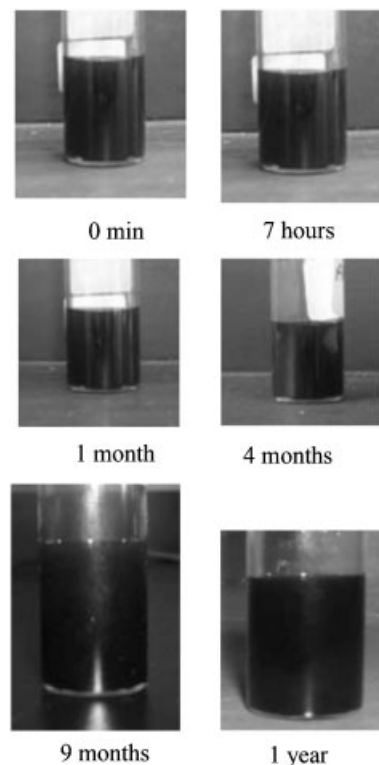


Figure 1. Digital images of DWNT/PVDF-DMAC solutions as a function of time. The solutions contain 0.05 wt.-% DWNTs and 14.95 wt.-% PVDF in DMAC.

researchers have demonstrated a donor acceptor interaction mechanism between CNTs and PVDF, and they further suggested that the interaction involves the fluorine in the PVDF structure.^[16] Consequently, we attribute the observed dispersion stability in our solutions to a non-covalent interaction between the nanotubes and the PVDF. Figure 2 shows an SEM image of 2.28 vol.-% DWNT in PVDF. SEM images are taken on freeze-fractured surfaces. Figure 2a shows DWNT bundles well dispersed throughout the composite. A higher magnification of the fracture surface (Figure 2b) is used to estimate the average diameter of the DWNT bundles. The average diameter of the thicker bundles is found to be 23 ± 2.56 nm while the thinner bundles have an average diameter of 11 ± 1.86 nm. Figure 2c shows a higher DWNT volume content in PVDF, illustrating good dispersion even at higher concentration. At higher magnification (Figure 2d), an average diameter of 12 ± 2.53 nm is observed.

Electrical Conductivity and Dielectric Spectroscopy

Figure 3 shows the electrical conductivity for varying volume percent of DWNT as a function of frequency in PVDF. At a particular frequency an increase in the conductivity is seen as the volume fraction increases.

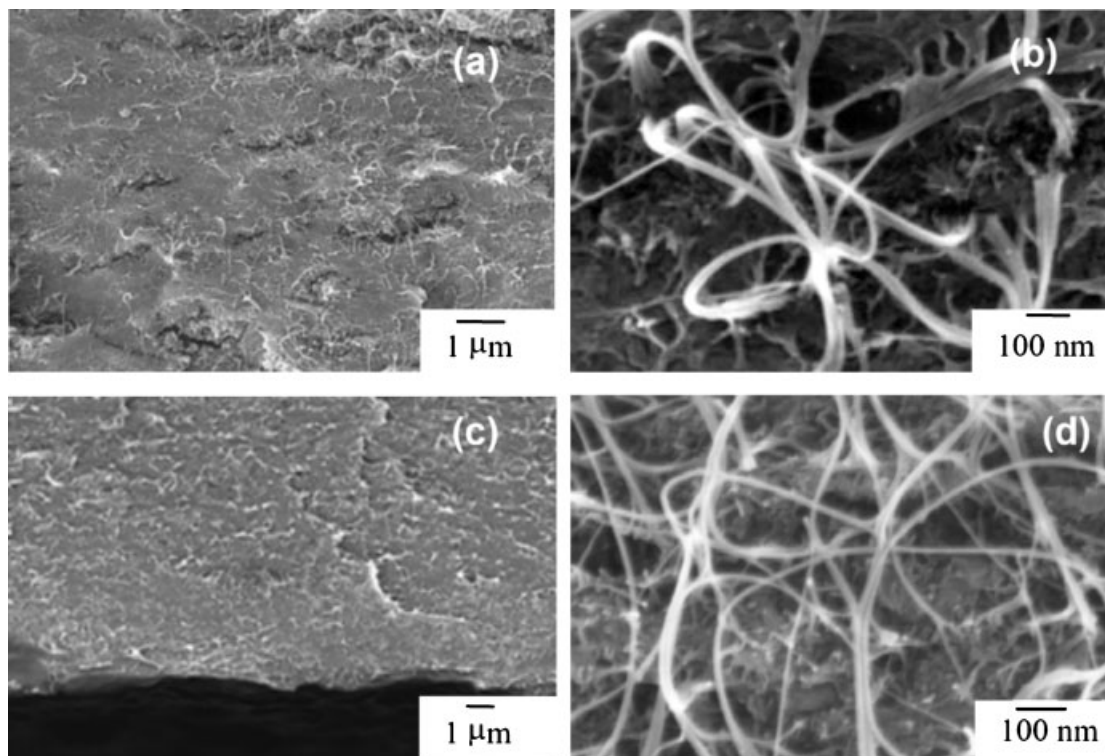


Figure 2. SEM images of 2.28 vol.-% DWNT/PVDF sample (a) scale bar 1 μm, (b) scale bar 100 nm. (c) SEM images of 4.51 vol.-% DWNT/PVDF sample; scale bar 1 μm, (d) scale bar 100 nm.

Also, there are two different regions. The first region, where the AC conductivity is highly dependent on the frequency, extends from 0 to 0.23 vol.-% DWNT and is indicative of an insulator behavior. The second region, where the AC conductivity is independent of frequency, extends from 0.46 up to 4.5 vol.-%. In this region, a

continuous path of nanotubes has formed, making the composite conductive.

To better analyze the insulator-conductor transition, the DC electrical conductivity ($f=0$ Hz) data is extrapolated from the AC data and plotted against the volume fraction of the DWNT, as shown in Figure 4. A sharp increase is observed between 0.20 and 0.40 vol.-%, where the conductivity changes by 9 orders of magnitude, (from 1.29×10^{-12} to $3 \times 10^{-3} \text{ S} \cdot \text{cm}^{-1}$). In addition, a plateau is reached above 0.57 vol.-% DWNT. Based on Figure 4, the percolation in this composite occurs between 0.20 and 0.40 vol.-%. In other words, below this concentration the material is very resistant to electron flow, while higher than this value the material is conductive. The dependence of DC conductivity (σ_{DC}) on the volume fraction of the nano-inclusions near the percolation threshold, p_c , is given by a power law relation given in Equation (1).^[5]

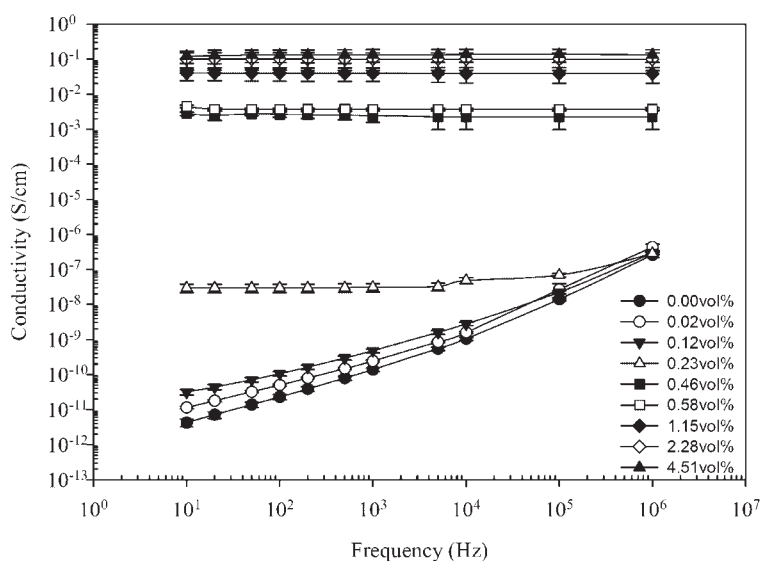
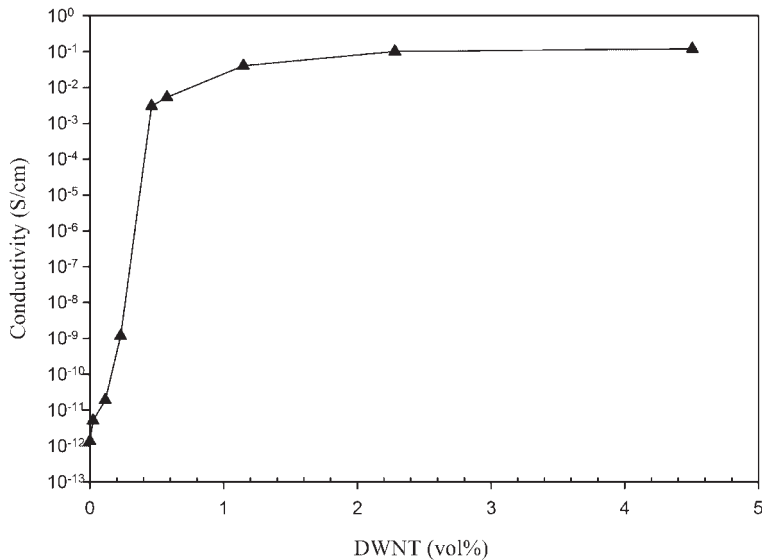


Figure 3. Electrical conductivity as a function of frequency for varying DWNT concentration.

$$\left\{ \begin{array}{l} \sigma_{DC}(p) \propto (p_c - p)^{-s}, p < p_c \\ \sigma_{DC}(p) \propto (p - p_c)^t, p > p_c \end{array} \right\} \quad (1)$$

These two expressions define two regions; one region below the percolation threshold concentration and the other region above the percolation threshold. A best fit to the experimental



■ Figure 4. DC conductivity as a function of DWNT concentration.

data identifies a percolation threshold value p_c of 0.23 vol.-% (0.19 wt.-%) with 1.91 as the exponent t . The value of exponent t is in agreement with values found in the literature for a three-dimensional dispersion model.^[18,19] Weber et al. discussed the value of t on the basis of percolation theory where the range varied from 1.2 to 2.0 depending on whether it is calculated in two or three dimensions.^[18] Gingold et al. reported a value of the exponent equal to 2.003 ± 0.047 assuming a three dimensional model.^[19]

Predicted percolation can be calculated assuming the ratio between the radius and the length of the tubes (r/l) is much less than 1.^[6] This assumption is met since, in case of the DWNTs in this work, the ratio r/l is less than or equal to 0.0075. The volume fraction at percolation is given in Equation (2):^[6]

$$p_c = \frac{\rho_c V_{\text{cyl}}}{V_{\text{tot}}} \quad (2)$$

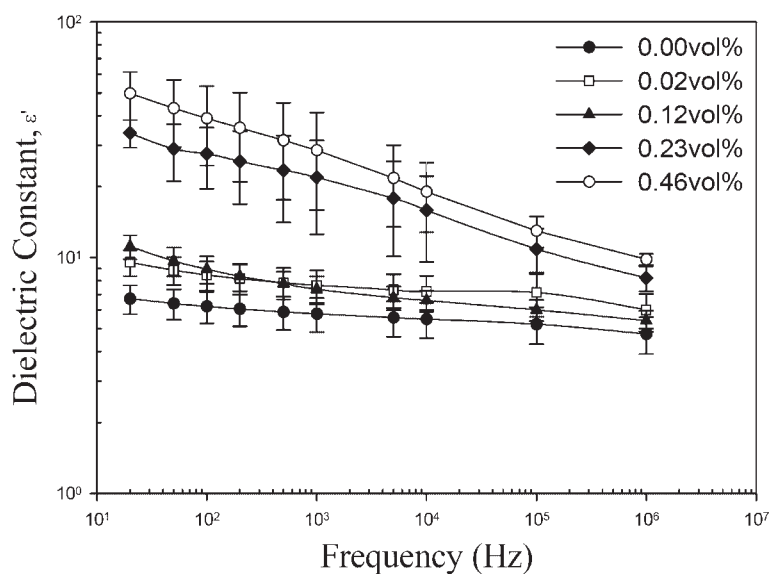
where p_c is the volume fraction at percolation, ρ_c is the percolation threshold, V_{cyl} is the volume of the particle which is treated as a capped cylinder, and V_{tot} is the total volume of the sample. The percolation threshold (ρ_c) is inversely proportional to the excluded volume (V_{ex}) which can be calculated as shown in Equation (3):

$$V_{\text{ex}} = \frac{32}{3}\pi r^3 + 8\pi r^2 l + 4l^2 r \sin \Theta \quad (3)$$

where r and l are the radius and the length of the tube, respectively and Θ is the angle between two tubes which ranges between $\pi/4$ for the isotropic and 0 for aligned samples. If ρ_c is to be inversely proportional to V_{ex} the isotropic case should be assumed. The thickness of films used is $\approx 35 \mu\text{m}$, which is normalized to 1. Using this analytical method, a percolation p_c of 0.069 vol.-% is predicted assuming that the DWNTs are individually dispersed (i.e., completely exfoliated). However, SEM images show that the dispersion consists of thin bundles or ropes. Recalculating p_c by assuming that the bundles consist of 7 tubes forming a hexagonal arrangement yields a predicted percolation value of 0.20 vol.-%, which is very close to the experimentally determined value of 0.23 vol.-%. The diameter of the bundles in this case is 9 nm which is also very close to the calculated diameter from the SEM images of 12 nm. Recalculating p_c by assuming that the bundles consist of 19 tubes, the resultant p_c is 0.33%.

Therefore, the experimental results lie between 7 cylinders and 19 cylinders of DWNTs.

Figure 5 shows the dielectric constant versus frequency for varying DWNT concentration in PVDF. It is seen that at any particular frequency the dielectric constant increases as the volume percent increases. It is not possible to measure reasonable values for dielectric constant for high volume fraction due to the increased electrical conductivity of the material. At frequencies below 500 Hz and DWNT volume contents above 0.46 vol.-%, the measured



■ Figure 5. Dielectric constant as a function of frequency for composites with varying DWNT concentration.

capacitance values are negative. It is seen that the curves in Figure 5 can be divided into two regions. The first region is for the low volume contents, between 0 and 0.12 vol.-% DWNTs. The values of the dielectric constant are close to each other (between 7 and 10) and they do not vary greatly with frequency. The second region is for samples with higher volume content. In this region, the dielectric constant decreases more significantly with increasing frequency.

Thermomechanical Behavior

DSC was used to study the thermal transitions within PVDF containing 0 to 4.51 vol.-% DWNT. The T_m , T_c , enthalpy, and the percent crystallinity were estimated from the DSC curves. Pure PVDF powder has a melting temperature range from 155 to 165 °C, low crystallinity, and high molecular weight. Table 2 presents T_m , T_c , and the degree of crystallinity in the DWNT/PVDF nanocomposites. The T_m of the as-cast PVDF is about 162.1 °C and the crystallization temperature is around 133 °C. The T_m for 4.51 vol.-% DWNT/PVDF is about 161 °C, and the T_c is around 139 °C. In general, there is no large difference in T_m between the neat PVDF and the various nanocomposites. The T_m is used as a technique to determine whether there is a transformation between the four phases of PVDF; some researchers show a transformation between PVDF phases, especially α -phase to β -phase, by using the T_m as a criterion for this transformation.^[14] The lower melting temperature is due to the formation of α -phase crystalline structure; while the high melting peak is due to the formation of β -phase. Based on the lack of significant change in T_m , our results indicate that it is unlikely that phase transformation takes place with the addition of DWNTs. Our preliminary X-ray diffraction characterization points to the same conclusion, where no evidence of β -phase is observed.

The second column in Table 2 shows the T_c ; the PVDF nanocomposites crystallize at higher temperature than the neat PVDF. This increase in T_c reveals the impact of the DWNTs on the crystallization kinetics of PVDF, namely it indicates the high nucleation ability of the DWNTs. In general, the T_c difference between the neat PVDF and the samples containing DWNT is 4–8 K; for example, 4.51 vol.-% DWNT crystallizes at 138.9 °C while neat PVDF crystallizes at 132.6 °C. Table 2 also shows that the heat of fusion and the percent crystallinity decrease as the DWNT volume content increases in the composites. The heat of fusion of PVDF decreased from 37.9 for PVDF to 24.4 J · g⁻¹ for 4.51 vol.-% DWNT in PVDF. The decrease in the heat of fusion points to an overall lower crystallinity in the PVDF composites. The percent crystallinity of the PVDF is calculated assuming a value of the heat of fusion of 104 J · g⁻¹ for 100% crystalline PVDF; the crystallinity of PVDF decreases from 36.5 for neat PVDF to 23.5% for 4.51 vol.-% DWNT/PVDF. Therefore, although the DWNTs act as nucleating agents, the overall percent crystallinity of the DWNT/PVDF composites is lower than that of the neat PVDF. The rate of crystallization and resulting percent crystallinity are affected by both the number of nucleation sites as well as their ability to grow. We surmise that, in the PVDF system, though the DWNTs act as nucleation sites, the strong interaction between the nanotubes and the PVDF coupled with the high aspect ratio of the DWNTs impede crystal formation by confining the polymer chains. A similar effect of CNTs on polymer crystallinity is seen in the recent literature.^[20,21] We are currently pursuing isothermal studies, where the temperature is maintained for a few minutes between T_m and T_c to explore the promotion of crystallization in the presence of DWNTs under those conditions.

Figure 6 shows the storage modulus of PVDF nanocomposites as a function of temperature. PVDF nanocomposites in general show an increase in the storage modulus over the entire temperature range as compared to the neat

Table 2. T_m , T_c , ΔH and percent crystallinity of DWNT/PVDF composites.

Sample Name	T_m	T_c	ΔH	Crystallinity
	°C	°C	J · g ⁻¹	%
0 vol.-% DWNT/PVDF	162.1	132.6	37.9	36.5
0.02 vol.-% DWNT/PVDF	163.9	136.6	37.8	36.3
0.12 vol.-% DWNT/PVDF	162.9	139.6	36.5	35.1
0.23 vol.-% DWNT/PVDF	161.9	136.8	36.3	34.9
0.46 vol.-% DWNT/PVDF	163.4	139.9	36.1	34.7
1.15 vol.-% DWNT/PVDF	163.5	139.9	34.1	32.8
2.28 vol.-% DWNT/PVDF	162.6	140.7	30.3	29.1
4.51 vol.-% DWNT/PVDF	161.1	138.9	24.4	23.5

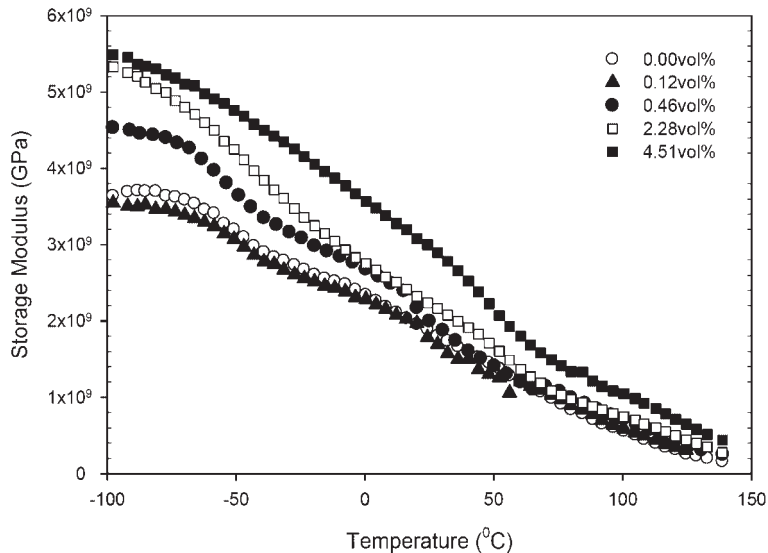


Figure 6. Temperature dependence of the storage modulus for PVDF/nanocomposites.

Table 3. Ratio of values for comparison at different temperatures.

Sample Name	E'_{c}/E'_{p}		
	$T = -90^{\circ}\text{C}$	$T = 40^{\circ}\text{C}$	$T = 100^{\circ}\text{C}$
0.12 vol.-% DWNT/PVDF	1.19	1.14	1.06
1.15 vol.-% DWNT/PVDF	1.68	1.29	1.27
2.28 vol.-% DWNT/PVDF	1.79	1.49	1.30
4.51 vol.-% DWNT/PVDF	1.84	1.97	1.83

PVDF. Also, the storage modulus increases with an increase in the DWNT content. The increase in storage modulus can be explained by the fact that a strong interfacial interaction exists between the PVDF and the DWNTs. The effectiveness of DWNT as a reinforcement is highlighted in Table 3 where the increase in the storage modulus of the nanocomposites is expressed in terms of the ratio of the modulus of the composites to the modulus of the neat PVDF. At low DWNT volume concentration and at low temperature (-90°C), the increase is about 19%; however, at 100°C the increase is only about 8%. As the DWNT volume fraction increases to about 4.5 vol.-%, the E'_{c}/E'_{p} ratio significantly increases by more than 80%. At higher temperature (100°C), the increase is more pronounced to 1.83. The higher increase in the storage modulus in the elastic region (well above the T_g of PVDF) confirms the reinforcing effect of DWNT in the nanocompo-

sites. At very high volume fraction (4.51 vol.-%), a significant improvement relative to the neat PVDF is seen at all temperatures. The enhancement in storage modulus is due to the dispersion and high aspect ratio of the double-walled carbon nanotubes.

Figure 7 shows the $\tan \delta$ curves of PVDF and DWNT/PVDF nanocomposites. The $\tan \delta$ curves show a broad peak near -50°C for PVDF and the DWNT/PVDF composites, which corresponds to the T_g of PVDF. No change in the T_g is observed by adding the DWNTs, which may be explained by the fact that the DWNTs, acting as nucleation sites, are preferentially present in the crystalline regions as discussed above. In this case, they influence the crystallites rather than the amorphous region which is responsible for T_g .

Electromechanical Behavior

Figure 8 presents the actuation strain results for samples containing 0.23, 2.28 and 4.51 vol.-% DWNT, using the cantilever bending experiment under a DC electric field. It is noted that nanocomposite samples below the percolation threshold (less than 0.23 vol.-% DWNTs) do not show any actuation response and the actuation response gets stronger as the nanotube content increases. There is an increase in strain and a decrease in the applied electric field (E) as DWNT content increases from 0.23 to 2.28 vol.-%. At 4.51 vol.-%, initially strain is observed at a lower electric field, as low as $14 \text{ kV} \cdot \text{m}^{-1}$. However, as the field is increased to $22 \text{ kV} \cdot \text{m}^{-1}$, no further strain is observed, possibly due to the increased electrical

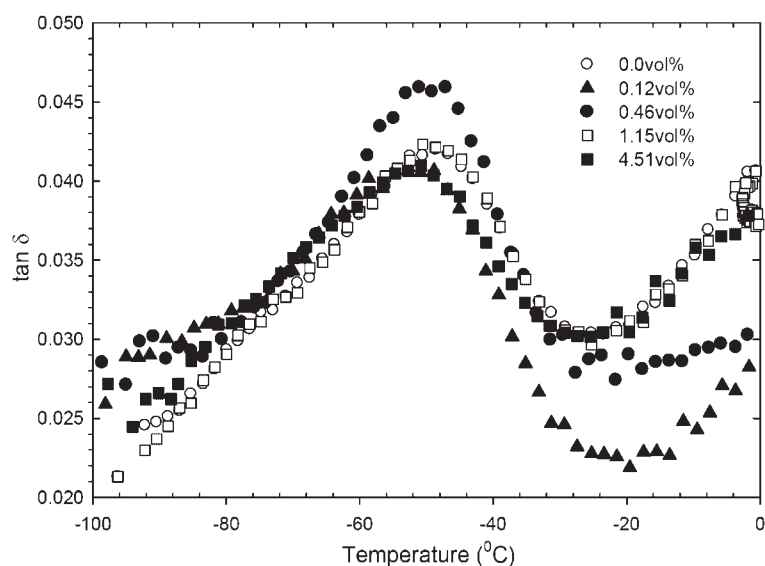


Figure 7. $\tan \delta$ as a function of temperature for PVDF and DWNT/PVDF composites.

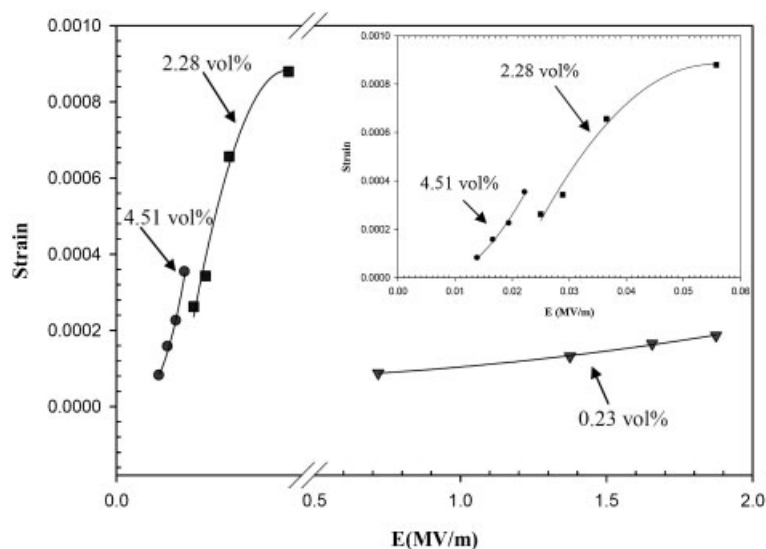


Figure 8. Strain versus (DC) electric field for varying DWNT concentration in PVDF.

conductivity of the composite at this concentration. The mechanism of actuation is believed to result from the nanotubes acting as local electrodes, effectively increasing the local field and resulting in a higher polarization at a given applied field. It is possible that there is also an increase in the induced dipoles due to DWNT/PVDF interaction. Future work is focusing on identifying the mechanism(s) responsible for strain actuation at low fields in the DWNT/PVDF composites.

Conclusion

DWNT/PVDF composites are prepared to assess the quality of nanotube dispersion and the resulting physical properties. The results show that the dispersion of DWNT is good and the procedure followed for dispersing the nanotubes yields a stable solution over a long period of time (>1 year). SEM images show a good dispersion of small DWNT bundles in the PVDF matrix. These images were used to estimate the diameter of the DWNT bundles. In these composites, bundles of 15–22 nm are observed. Correlating the percolation estimated using electrical conductivity and that estimated using the excluded volume approach suggests a bundle size of 7 tubes in a hexagonal arrangement. This would correspond to a bundle diameter of ≈ 15 nm, which is consistent with the SEM results. The effect of the DWNT on the PVDF morphology was also studied using DSC. A decrease in the percent crystallinity and an increase in the T_c are observed as the DWNT concentration increases, indicating that, while the DWNTs act as nucleation sites, their strong interaction with the PVDF chains impedes crystal growth and therefore

interferes with crystallization. Electrical conductivity measurements were used to assess the percolation transition, but also highlighted the effect of DWNTs on the electrical properties of PVDF. The relationship between electrical conductivity and frequency shows two regions, one for the higher volume content (from 0.23 to 4.51 vol.-% DWNT) with a constant electrical conductivity and the other (from 0 to 0.23 vol.-% DWNT) with a frequency dependence, which is typical of insulators. The electrical conductivity increases from 10^{-12} S \cdot cm $^{-1}$ for neat PVDF to 10^{-1} S \cdot cm $^{-1}$ for 4.51 vol.-% DWNT. Similarly, the relationship between dielectric constant and frequency shows two different regions, one with low DWNT concentration that is independent of frequency, and another with frequency dependence. The storage modulus increases by 48% below T_g and by more than 85% above it at 4.5 vol.-% DWNT. Electromechanical characterization indicates an effect of DWNTs on the PVDF

dipolar interaction, where an increase in the electroactive performance is measured; possibly due to an enhanced local field in the presence of DWNTs. As the DWNT content in the PVDF is increased, we observed: 1) an increase in electric field-induced strain; and 2) a decrease in the electric field required to initiate a measurable strain. These findings highlight the potential of CNTs to improve the performance of electroactive polymers by addressing their current shortfalls such as high actuation voltage and low electric field-induced strain.

Acknowledgements: Z. O. and J. G. would like to acknowledge financial support from the *National Science Foundation* (NSF) under grant numbers CMMI-0514265 (Z. O.) and CMMI-0644055 (J. G.).

Received: July 26, 2007; Revised: November 3, 2007; Accepted: November 6, 2007; DOI: 10.1002/mame.200700229

Keywords: dielectric properties; differential scanning calorimetry (DSC); double-walled carbon nanotubes (DWNT); mechanical properties; nanocomposites

- [1] M. Moniruzzaman, K. Winey, *Macromolecules* **2006**, *39*, 5194.
- [2] E. Thostenson, L. Chunyu, T. Chou, *Compos. Sci. Technol.* **2005**, *65*, 491.
- [3] K. Putz, C. Mitchell, R. Krishnamoorti, P. Green, *J. Polym. Sci., Part B: Polym. Phys.* **2004**, *42*, 2286.
- [4] F. Gojny, M. Wichmann, U. Köpke, B. Fiedler, K. Schulte, *Compos. Sci. Technol.* **2004**, *64*, 2363.
- [5] P. Petra, S. Dudkin, I. Alig, *Polymer* **2003**, *44*, 5023.
- [6] Z. Ounaies, C. Park, K. Wise, E. Siochi, J. Harrison, *Compos. Sci. Technol.* **2003**, *63*, 1637.

- [7] F. Liang, J. Beach, P. Rai, W. Guo, R. Hauge, M. Pasquali, R. Smalley, W. Bilups, *Chem. Mater.* **2006**, *18*, 1520.
- [8] C. Dyke, J. Tour, *J. Phys. Chem.* **2004**, *108*, 11151.
- [9] Y. Wang, Z. Iqbal, S. Mitra, *J. Amer. Chem. Soc.* **2006**, *128*, 95.
- [10] J. Grunlan, L. Liu, Y. Kim, *Nano. Lett.* **2006**, *6*, 911.
- [11] V. Moore, M. Strano, E. Haroz, R. Hauge, R. Smalley, J. Schmidt, Y. Talmon, *Nano. Lett.* **2003**, *3*, 1379.
- [12] M. O'Connell, P. Boul, L. Ericson, C. Huffman, Y. Wang, E. Haroz, C. Kuper, J. Tour, K. Ausman, R. Smalley, *Chem. Phys. Lett.* **2001**, *342*, 265.
- [13] K. Wise, C. Park, E. Siochi, J. Harrison, *Chem. Phys. Lett.* **2004**, *391*, 207.
- [14] R. G. Kepler, "Ferroelectric, Pyroelectric, and Piezoelectric Properties of Poly(vinylidene Fluoride)", in: *Ferroelectric Polymers: Chemistry, Physics, and Applications*, 1st edition, H. S. Nalwa, Ed., Marcel Dekker, New York 1995, p. 183–232.
- [15] H. Kawai, *Jpn. J. Appl. Phys.* **1969**, *8*, 975.
- [16] F. J. Owens, J. R. P. Jayakody, S. G. Greenbaum, *Compos. Sci. Technol.* **2006**, *66*, 1280.
- [17] C. Park, Z. Ounaies, K. Watson, R. Crooks, J. Smith, Jr., S. Lowther, J. Connell, E. Siochi, J. Harrison, T. St. Clair, *Chem. Phys. Lett.* **2002**, *364*, 303.
- [18] M. Weber, M. Kamal, *Polym. Compos.* **1997**, *18*, 711.
- [19] D. Gingold, C. Lobb, *Phys. Rev. B* **1990**, *42*, 8220.
- [20] S. Li, Z. Li, M. Yang, Z. Hua, X. Xu, R. Huang, *Mater. Lett.* **2004**, *58*, 3967.
- [21] L. Valentini, J. Biagiotti, M. Lopez-Manchado, S. Santucci, J. Kenny, *Polym. Eng. Sci.* **2004**, *44*, 303.